Toxicity and DNA repair in normal human keratinocytes co-exposed to benzo[a]pyrene and sunlight

Anne von Koschembahr, Antonia Youssef, David Béal, Leslie Gudimard, Jean-Philippe Giot, Thierry Douki

Toxicity and DNA repair in normal human keratinocytes co-exposed to benzo[a]pyrene and sunlight

Anne von Koschembahr[1], Antonia Youssef[1], David Béal[1], Leslie Gudimard[1], Jean-Philippe Giot[2], and Thierry Douki[1,*]

[1] Univ. Grenoble Alpes, SyMMES/CIBEST UMR 5819 UGA-CNRS-CEA, INAC/CEA-Grenoble LAN, F-38000 Grenoble

[2] Service de Chirurgie Plastique et Maxillo-faciale, Centre Hospitalier Universitaire Grenoble Alpes, La Tronche, France

[*]Corresponding author: Thierry Douki

INAC/SyMMES/CIBEST, UMR 5819 UGA-CNRS-CEA

CEA-Grenoble

17 avenue des Martyrs

38054 Grenoble Cedex 9

France

Telephone: +33 4 38 78 31 91

Fax: +33 4 38 78 50 90

Email: thierry.douki@cea.fr

Abstract

Skin has the potential to be exposed to both solar UV radiation and polycyclic aromatic hydrocarbons, especially in occupational environments. In the present work, we investigated how benzo[a]pyrene (B[a]P) modulates cellular phototoxicity and impacts formation and repair of pyrimidine dimers induced by simulated sunlight (SSL) in normal human keratinocytes (NHK). We were especially interested in determining whether the aryl hydrocarbon receptor (AhR) was involved since it was recently shown to negatively impact repair. Addition of 1 µM B[a]P after exposure to 2 minimal erythemal doses of SSL had little impact on NHK. The inverse protocol involving incubation with B[a]P followed by irradiation led to a strong increase in phototoxicity. Repair of DNA photoproducts was drastically impaired. Using agonists and antagonists of AhR allowed us to conclude that this factor was not involved in these results. Observation of a strong increase in the level of the oxidative marker 8-oxo-7,8-dihydroguanine in the protocol involving B[a]P treatment followed by exposure to SSL strongly suggested that a photosensitized oxidative stress was responsible for cell death and inhibition of DNA repair. Accordingly, both adverse effects were diminished with a lower concentration of B[a]P and a lower SSL dose, leading to less oxidative stress.

Keywords: Human skin; sunlight; DNA damage; polycyclic aromatic hydrocarbons; co-exposure; keratinocytes

Graphical Abstract

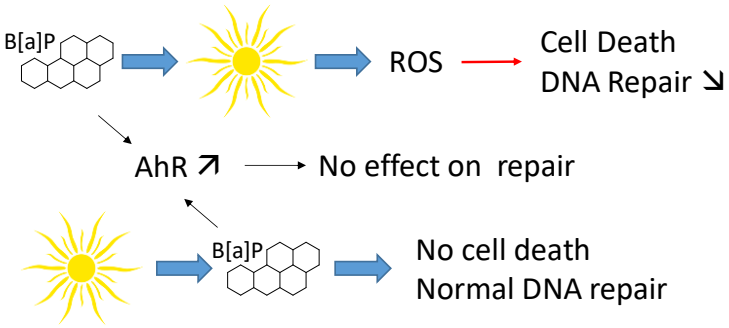

Incubation of human keratinocytes with B[a]P before exposure to simulated sunlight increased cell death and hampered DNA repair. The opposite protocol had no effect on these two endpoints. A significant contribution of AhR activation was ruled out, while photo-oxidative stress was proposed to play a major role under the former experimental conditions.

1. Introduction

Skin cancer is a major health concern. A large amount of experimental and epidemiological studies have shown the involvement of overexposure to solar UV radiation (Melnikova and Ananthaswamy, 2005; Molho-Pessach and Lotem, 2007). UV photons, in particular UVB, are absorbed by DNA where they induce the formation of cyclobutane pyrimidine dimers (CPD), pyrimidine (6-4) pyrimidone photoproducts (64PP), and their Dewar valence isomers (Cadet et al., 2005). Bipyrimidine photoproducts are responsible for the mutations found in skin tumors, which are mostly encountered at bipyrimidine sequences (Brash, 2015; Brash et al., 1991; Ziegler et al., 1993). Solar light is not the only genotoxic agent to which skin is exposed. Indeed, chemicals can interact with skin and cause deleterious effects. Polycyclic aromatic hydrocarbons (PAH) are among these toxic compounds to which workers may be cutaneously exposed (Bonzini et al., 2013; Cirla et al., 2007; Herbert et al., 1990; Sellappa et al., 2011; Serdar et al., 2012; Vaananen et al., 2005). PAH are by-products of the combustion of organic matter and are thus found in many products used in industry or released by numerous industrial processes. Among other deleterious health effects, PAH are suspected of exhibiting genotoxic and carcinogenic effects in skin (Boffetta et al., 1997).

The toxicity and genotoxicity of PAH in skin has been well investigated, but a complete understanding of the cutaneous impact of these compounds has to include their co-exposure with sunlight, in particular the UV portion of its spectrum. Workers who conduct their occupational activities outdoors (i.e., roofers, road construction crew) can be simultaneously exposed to solar radiation and PAH. Workers exposed to PAH indoors may be exposed to sunlight following the working hours, for instance during recreational activities. In addition to these concerns for occupational safety, the role of co-exposure to PAH and sunlight has been recently pointed out in the general population (Marrot, 2018; Zegarska et al., 2017). Therefore,

a precise understanding of biological processes impacted by simultaneous exposure to PAH and sunlight is mandatory to propose an efficient protection strategy.

A first possible mechanism is a phototoxicity effect driven by photosensitized reactions and oxidative stress. This aspect has been well studied *in vitro* (Crallan et al., 2005; Mauthe et al., 1995; Soeur et al., 2017; Yu et al., 2006). An additional role of solar UV could be the conversion of parent PAH into more toxic photodegradation products (Teranishi et al., 2010; Toyooka and Ibuki, 2007). An *in vivo* experiment has also shown that co-exposure of mice to UVA and B[a]P increased the level of DNA adducts in skin, possibly as the result of their impaired repair (Saladi et al., 2003). A link with cancer could also be that both B[a]P and UV modulate cell proliferation (Pandey et al., 2018).

Another pathway linking PAH and UV exposure involves the aryl hydrocarbon receptor (AhR). This important factor in the cellular response to xenobiotics is essential for the triggering of the metabolism machinery and is activated by binding to compounds, such as dioxins and PAH. Interestingly, UV radiation has also been shown to induce the activation of AhR and trigger a wide variety of biological responses (Esser et al., 2013; Rannug and Fritsche, 2006). Among them is the activation of the xenobiotic metabolism pathway and the overexpression of CYP450 enzymes (Fritsche et al., 2007; Nair et al., 2009). This effect was proposed to be mediated by endogenous tryptophan photoproducts and, in particular, 6-formylindolo[3,2-b]carbazole (FICZ), which has been detected in irradiated cells only after incubation with very high, non-physiological concentrations of tryptophan (Fritsche et al., 2007) but not under more biologically relevant conditions (Youssef et al., 2018). The origin and the extent of this stimulation of metabolization remain thus to be assessed. In contrast to what was expected, we recently reported that simulated sunlight (SSL) applied to primary cultures of human keratinocytes or skin explants reduced the B[a]P-induced expression of CYP450 and the level of the B[a]P diol epoxide adducts in DNA (von Koschembahr et al., 2018). Similar results were

obtained for the production of metabolites in skin co-exposed to complex PAH mixtures and SSL (Bourgart et al., 2019). The extent of AhR stimulation by sunlight in the presence of PAH is thus an important issue in understanding the toxic and genotoxic effects of co-exposures in skin, particularly since AhR was recently reported to exhibit a negative impact on DNA repair (Pollet et al., 2018).

The present work was thus designed to explore the impact of the presence of B[a]P on the deleterious effects of SSL in primary culture of human normal keratinocytes (NHK). We previously studied the modulation of PAH metabolism and DNA damaging properties of B[a]P in the same biological model (von Koschembahr et al., 2018). Here, we focused on cytotoxicity and formation and repair of UV-induced pyrimidine dimers. Emphasis was placed on the possible role played by AhR.

2. Material and methods

2.1 Culture of primary human keratinocytes

Keratinocyte cultures were prepared from fresh human skin samples, as previously described (Mouret et al., 2006). Human skin samples were obtained according to the French Public Health Code on the use of surgical waste (article L1245-2). Donors were healthy females undergoing elective breast reduction surgery (Centre Hospitalier Universitaire de Grenoble, Grenoble, France) who gave their informed consent. All experiments were performed in accordance with relevant guidelines and regulations. Storage of human skin samples was listed in the CODECOH DC-2019-3391 document validated by the appropriate authorities. Donors were between the ages of 17-58, and their skin were phototypes II or III of the Fitzpatrick classification (Fitzpatrick, 1988). NHK were grown in keratinocyte serum-free medium (KSFM) containing 1% Pen/Strep, 25 µg/mL bovine pituitary extract (BPE), and 0.9 ng/mL of recombinant human epidermal growth factor (EGF). BPE and EGF were removed from the cell

culture media 24 hours before B[a]P treatments or irradiations, and throughout the subsequent experiment.

2.2 Treatment of keratinocytes

Protocols involved exposure to SSL and/or treatment by B[a]P. Exposures to SSL were performed with a LS1000 Solar Simulator (Solar Light Company, Glenside, PA), which emitted wavelengths in the 290-400 nm range. The radiation intensity was 22 J cm^{-2} h^{-1} corresponding to 6 minimal erythema doses (MED) per hr. The maximal SSL dose used was 2 MED. B[a]P (Sigma-Aldrich) diluted in DMSO at 10 mM was added to the culture medium to reach the final targeted concentration which ranged between 0.05 and 2 µM depending on the experiments. For the SSL/B[a]P protocol, keratinocytes were rinsed twice with PBS and exposed to 2 MED SSL in PBS. They were then maintained in PBS in the incubator for 1 hour. PBS was removed, and KFSM with or without B[a]P diluted in DMSO was added to reach the final targeted concentration. Samples were collected after increasing periods of time. Controls were incubated with medium containing pure DMSO. For samples treated under the B[a]P/SSL protocol, medium containing 1 µM or less B[a]P was added to the cells. The samples were then maintained in the incubator. Twenty-four hours later, culture medium was removed and the samples rinsed twice with PBS. Similar pre-treatments were performed with medium containing either 1µM B[a]P and the AhR antagonist CH223191 (concentrations from 2 to 25 µM in DMSO) or 2,3,7,8-Tetrachlorodibenzo-p-dioxine (TCDD, concentrations from 2 to 25 nM in toluene). SSL irradiations were performed in PBS, and NHK were placed back in culture medium with or without B[a]P. Cell pellets were collected as technical quadruplicates using biological replicates after increasing periods of time and frozen at -20°C. UVB irradiation was performed like exposure to SSL with a 2x15 W UVB lamp (VL-245G, Bioblock) exhibiting an emission spectrum centered at 312 nm.

2.3 Determination of cellular toxicity in NHK

Cytotoxicity of the exposure to SSL and/or B[a]P was assessed from the measurement of mitochondrial activity by using the 3-[4,5-dimethylthiazol-2-yl]-2,5-diphenyl tetrazolium bromide (MTT) assay. NHK (20,000 cells per well) were grown in 96-well plates, and exposed to the chosen protocol in terms of B[a]P concentration and dose of SSL. Additionally, NHK were also exposed to CH223191 or TCDD in order to ensure the working concentrations did not have any major cytotoxic effects. After 24 or 48 hours, the exposure media were replaced with 100 µL of MTT solution and the plates were incubated 1 hour at 37°C. Formazan crystals were dissolved with 100 µL of DMSO. Absorption was then measured at 560 nm. Assays were reproduced three times with cells from three different donors independently, with n=6, i.e. 6 independent replicates in each independent experiment.

2.4 Clonogenicity

Cells were seeded at 20 cells/cm^2 and grown in 6-well plates (area 9.5 cm^2) for 24 hours before being exposed to B[a]P concentration and SSL dose at the chosen values. Irradiations were performed in PBS. Fresh medium was then added, which was changed every fourth day. When colonies in the control samples reached a cell content of approximately 50, namely around the 10^{th} day of culture, the medium was removed from all plates and a solution of crystal violet (0.5% in H_2O/EtOH 1:1) was added. After rinsing with water, the colonies were counted in each plate. Results were expressed in % with respect to controls.

2.5 Quantification of DNA damage

DNA was extracted from pellets containing 1 to 2 million cells using a protocol developed to limit spurious oxidation (Ravanat et al., 2002). DNA was recovered in 50 µl of a deferoxamine solution. DNA was subsequently hydrolyzed by a cocktail of enzymes, all purchased from Sigma-Aldrich. The first incubation was performed using phosphodiesterase II, DNase II, and

nuclease P1 (37°C, 2 hours). The second incubation step was then performed using phosphodiesterase I and alkaline phosphatase (37°C, 2 hours).

Samples were then injected on an HPLC system (ExionLC, SCIEX) equipped with a reverse-phase HPLC column (150 x 2 mm ID, 3 µm particle size, ODB, Interchim, Montluçon, France). The mobile phase was a gradient of acetonitrile (2 to 25 %) in 2 mM triethylammonium acetate (pH 6). CPDs, 64PPs, and Dewars from TT, TC, CT and CC dinucleotides were quantified on a tandem mass spectrometer (SCIEX QTrap 6500^{+}) as previously described (Douki, 2013). 8-Oxo-7,8-dihydro-2'-deoxyguanosine (8-oxodGuo) was quantified in the same samples in a second injection. The HPLC solvent was then a gradient of methanol in 2 mM ammonium formate and the monitored transition in positive ionization electrospray was m/z 284→168. HPLC-MS/MS was also used to quantify adducts between 2'-deoxyguanosine and B[a]P diol epoxide (BPDE-N^2-dGuo) using a previously described method (Genies et al., 2013; von Koschembahr et al., 2018). The mass spectrometer was used in the positive ionization mode and the monitored transitions were m/z 570→257 and m/z 570→454. The HPLC solvent was a gradient of acetonitrile in 2 mM ammonium formate. In all types of analyses, unmodified nucleosides were detected with a UV detector. External calibration of the response of the detector was performed for each run of analyses. Authentic standards were injected several times during the run and permitted to control the stability of the sensitivity of the detection and of the retention times. Results were expressed in number of DNA lesions per million normal bases.

2.6 Statistical analysis

Statistical analyses were performed on pools of replicates originating from different donors. Data were statistically analyzed in GraphPad PRISM using one-way ANOVA followed by application of the non-parametric Dunn's test for multiple comparisons.

3. Results

3.1 Short-term phototoxicity of co-exposure to B[a]P and SSL

Evaluation of the phototoxicity was based on the measurement of the mitochondrial activity, which relied on the MTT assay performed on NHK collected from three different donors. Experiments were repeated in biological triplicates for each of them. We first performed experiments where NHK were incubated with fixed B[a]P concentrations, namely 0.1 and 1 µM, and then exposed to increasing doses of SSL (B[a]P/SSL protocol, Fig. 1). The mitochondrial metabolic activity rapidly dropped with increasing SSL dose in NHK treated with 1 µM B[a]P. A similar trend was observed with 0.1 µM B[a]P, but the effect of the SSL dose was lower. An additional experiment was performed with keratinocytes exposed to 2 MED SSL in the presence of increasing concentrations of B[a]P (Supplementary data Fig. S1). B[a]P alone exhibited limited effect while the combined B[a]P/SSL treatment led to increased response already at 0.1 µM B[a]P. It may be added that little difference was observed between the mitochondrial activities of between untreated NHK and those submitted to SSL or B[a]P only (Fig. S1). No effect was observed for the SSL/B[a]P protocol, namely when SSL was applied before treatment with PAH. The values for the MTT assay were 82 ± 9 and 89 ± 12 % for the SSL and SSL/B[a]P protocols, respectively (n=3).

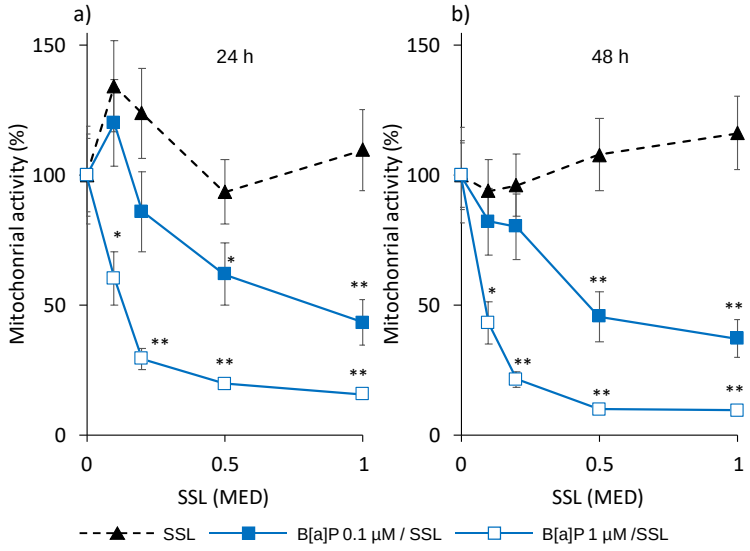

Figure 1: *Loss of mitochondrial activity in NHK exposed to increasing doses of SSL with irradiation performed after 24 hours of treatment with either 0.1 or 1 µM B[a]P. MTT assay was performed 24- and 48-hours following SSL exposure. Results are mean ± standard error obtained from three different donors. Statistical significance of the difference with respect to NHK exposed to SSL only: * p<0.05, ** p<0.01.*

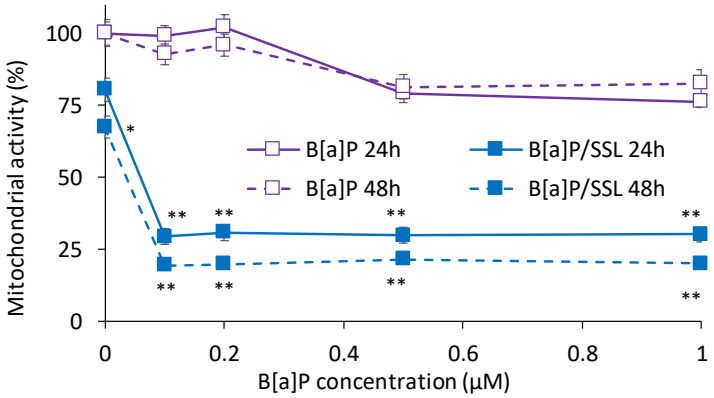

Figure S1: *Loss of mitochondrial activity in NHK exposed to increasing concentrations of B[a]P for 24 hours before being irradiated with 2 MED SSL. MTT assay was performed 24- and 48-hours following SSL exposure. Results are mean ± standard error obtained from three different donors. Statistical significance of the difference with respect to NHK exposed to B[a]P only: * p<0.05, ** p<0.01.*

3.2 Loss of clonogenicity in keratinocytes exposed to B[a]P followed by SSL irradiation

In order to better characterize the phototoxicity of co-exposure to SSL and B[a]P, we then performed a series of clonogenicity assays under our various experimental conditions. First, we studied the effect of exposure to pure B[a]P or exposure to SSL only. Under the most drastic conditions (1 µM B[a]P or 2 MED SSL), the clonogenicity was approximately 50% of that observed for untreated cells. It should be stressed that a stimulation effect was observed for the lowest doses of the two agents (Supplementary data Fig. S2). When cells were exposed to 2 MED of SSL after 24 hours of incubation with 1 µM of B[a]P, no colonies were detected in the plates. In contrast, when the converse protocol was applied (1 µM B[a]P after 2 MED SSL), the clonogenicity was roughly 70% of that of cells exposed to SSL only. In order to better characterize the impact of co-exposure to B[a]P and SSL, we repeated the experiments on lower ranges of B[a]P concentrations and SSL doses limited between 0.1 and 0.5 MED. As observed above, drastic effects were observed with the B[a]P/SSL protocol since no colonies were observed at 0.2 µM B[a]P with the 2 doses of SSL used, as well as at 0.2 µM with 0.1 MED (Fig. 2). In contrast, more colonies were detected under all conditions in the SSL/B[a]P protocol.

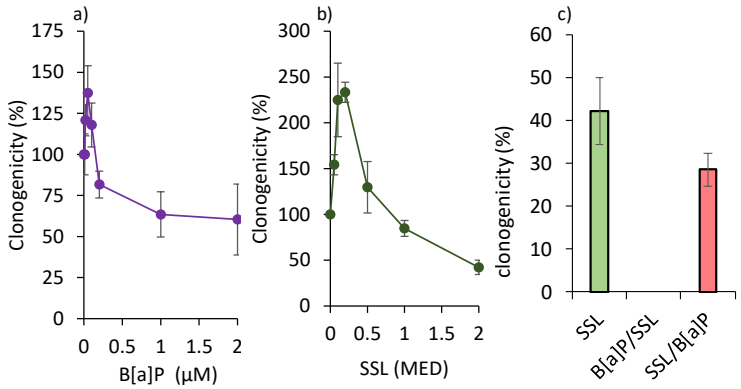

Figure S2: *Loss of clonogenicity observed in NHK exposed to a) increasing concentrations of B[a]P, b) increasing doses of simulated sunlight (SSL), and c) co-exposure to 1 µM B[a]P*

and 2 MED SSL following either the B[a]P/SSL or the SSL/B[a]P protocols. Results from two donors each studied in triplicate were pooled. Results represent the proportion of colonies with respect to vehicle-only treated controls. Reported data represent mean ± standard error (n=6).

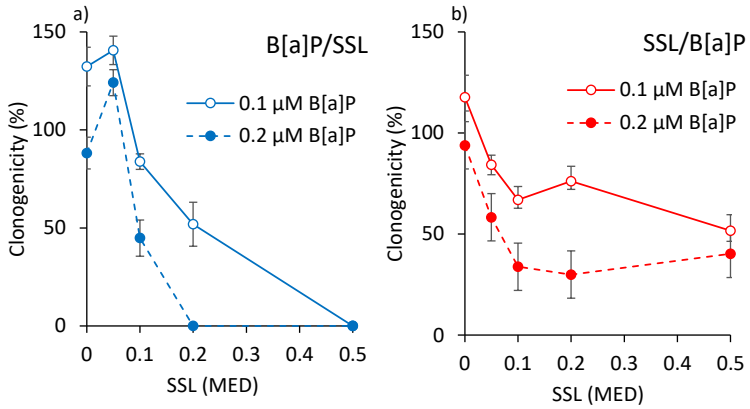

Figure 2: *Loss of clonogenicity observed in NHK exposed to increasing doses of SSL in combination with 0.1 or 0.2 µM B[a]P. The exposure conditions were either a) the B[a]P/SSL or b) the SSL/B[a]P protocols. Results from two donors each studied in triplicate were pooled. Results represent the proportion of colonies with respect to controls exposed to SSL without B[a]P. Reported data represent mean ± standard error (n=6).*

3.3 Impact of the addition of B[a]P on repair of DNA photoproducts

Since formation of DNA damage is a major cause of cell death, we quantified the level of all pyrimidine dimers in the various samples (Supplementary data, Table S1). Initial distribution of the photoproducts was similar under all conditions. CPDs were the most frequent photoproducts with the previously reported sequence effect (TT > TC > CT > CC). 64PPs were present in lower amounts and partly recovered as Dewar valence isomers. The latter observation is explained by the efficient conversion of 64PPs by the UVA component of SSL. A time-course study of our data showed that in samples exposed to SSL only, 64PPs and Dewars were

efficiently repaired. A difference was observed for the four CPDs, with TT CPD being the most slowly removed, while CC CPD was the fastest. These results are in line with previously published data (Mouret et al., 2008).

The addition of 1 µM B[a]P 1 hour after exposure to SSL did not modify the repair rate of CPDs (Fig. 3a). To eliminate a possible bias associated with the duration of the delay between irradiation and addition of B[a]P, we repeated the SSL/B[a]P treatment with a delay of 8 hours rather than the 1-hour time period previously used. Under both conditions, addition of B[a]P to the culture medium failed to modify the repair rate of neither CPDs nor 64PPs and Dewars (Supplementary data Fig. S3). In contrast, incubation of keratinocytes for 24 hours with B[a]P prior to exposure to SSL completely inhibited the repair of the three types of photoproducts (Fig. 3b). When UVB was used instead of SSL, no modulation of repair by B[a]P was observed, whether it was added before or after irradiation (Supplementary data Fig. S4).

Table S1: Level of pyrimidine dimers in NHK exposed to 2 MED SSL only or in combination with 1 µM B[a]P treatment. Results are expressed in number of photoproducts per millions bases and represent mean ± standard error.

time	TT CPD	TT 64PP	TT Dewar	TC CPD	TC 64PP	TC Dewar	CT CPD	CC CPD
SSL/B[a]P experiment								
SSL only								
0h	133.2±10.4	3.0±0.3	1.7±0.1	57.4±4.8	7.6±1.4	2.2±0.4	34.1±1.6	20.9±4.9
24h	95.4±10.1	0.7±0.2	0.0±0.0	39.3±7.2	2.8±0.9	0.0±0.0	12.2±2.6	19.3±6.2
48h	70.3±8.2	0.6±0.3	0.0±0.0	19.4±5.1	0.7±0.5	0.0±0.0	9.5±2.5	15.3±6.0
72h	76.3±9.2	0.2±0.1	0.0±0.0	20.1±6.6	0.4±0.2	0.0±0.0	6.4±1.5	9.8±5.2
SSL / B[a]P								
0h	131.9±8.1	2.1±0.6	1.3±0.3	55.5±5.3	5.9±2.3	1.3±0.3	34.4±1.5	24.9±2.4
24h	89.4±8.8	0.6±0.2	0.0±0.0	30.4±3.1	1.7±0.6	0.0±0.0	11.9±1.9	11.1±3.2
48h	89.2±12.9	0.3±0.2	0.0±0.0	21.3±4.5	0.5±0.0.3	0.0±0.0	8.5±1.6	12.3±4.6
72h	91.3±13.1	0.1±0.1	0.0±0.0	19.6±5.6	0.3±0.2	0.0±0.0	6.7±1.6	11.8±4.0
B[a]P/SSL experiment								
SSL only								
0h	111.0±14.8	2.5±0.3	1.1±0.1	71.2±17.4	10.9±1.2	2.6±0.7	30.4±3.5	13.8±2.0
24h	73.0±12.5	0.4±0.1	0.7±0.3	59.1±20.2	4.1±1.7	1.5±0.6	11.5±4.1	10.5±4.0
48h	48.5±12.8	0.7±0.4	0.1±0.0	43.9±20.0	0.3±0.1	0.6±0.3	8.4±3.8	8.9±4.2
72h	41.5±10.4	0.4±0.2	0.0±0.0	44.3±17.8	0.0±0.0	0.0±0.0	3.7±1.6	4.8±1.8
B[a]P / SSL								
0h	119.9±14.4	3.1±0.4	1.4±0.2	78.5±17.2	15.5±1.7	3.0±0.7	29.9±3.4	12.4±1.7
24h	119.6±15.4	2.5±0.3	1.2±0.2	76.9±19.3	13.8±1.7	3.6±1.0	33.6±3.9	13.7±2.3
48h	115.9±14.4	2.8±0.3	1.4±0.2	78.0±17.5	13.8±1.4	2.3±0.4	31.1±2.9	12.0±2.0
72h	107.9±14.8	2.6±0.3	1.4±0.3	79.2±16.7	13.8±1.6	4.5±1.6	31.6±3.2	15.3±2.2

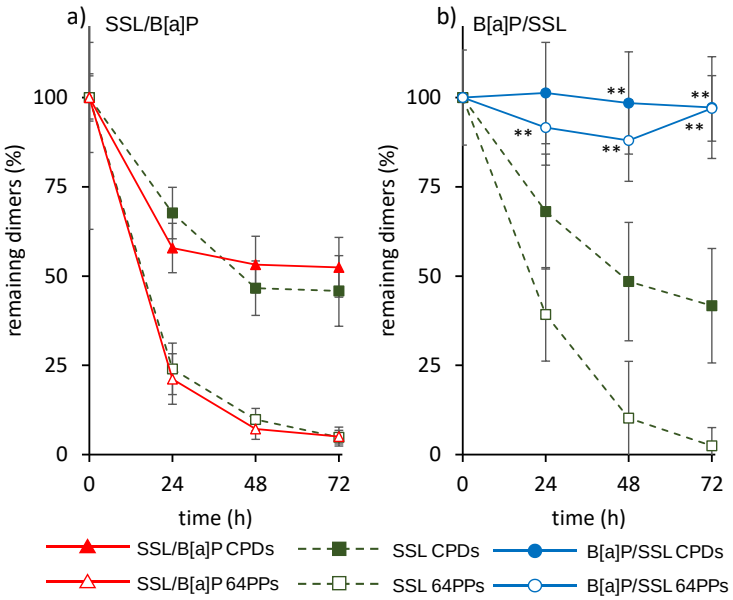

Figure 3: *Repair of pyrimidine dimers in NHK exposed to 2 MED SSL only or a) with a subsequent 1 µM B[a]P treatment performed 1 hour after irradiation, b) after a 24-hour preliminary incubation with 1 µM B[a]P. Results are the sum of either the level of the four CPDs or of TT and TC 64PPs and Dewars. Results were obtained from three donors each studied in three independent cultures. Data were normalized to 100 % for each donor and pooled. They are expressed in percentage of remaining lesions and represent mean ± standard error (n=9). Statistical significance with respects to SSL only *: $p<0.05$; **: $p<0.01$.*

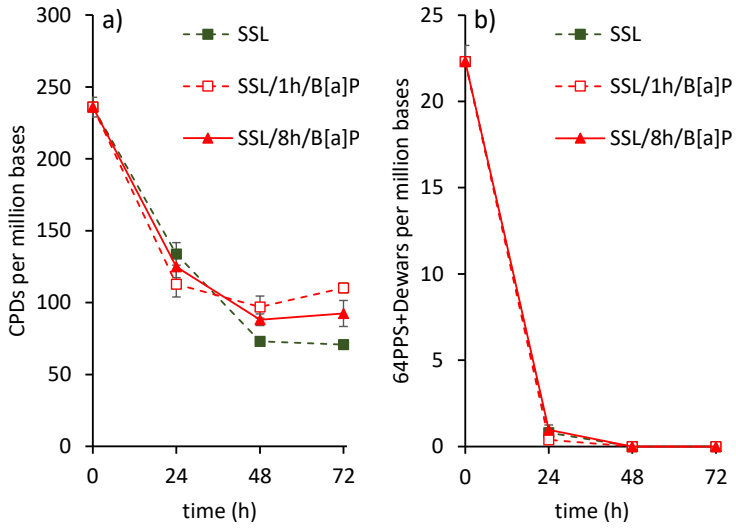

Figure S3: *Repair of pyrimidine dimers in NHK exposed to 2 MED SSL only or with a subsequent 1 µM B[a]P treatment performed 1 or 8 hours after irradiation. Data are shown for a) all 4 CPDs and, b) the TT and TC 64PPs and Dewars. Results from two donors each studied in triplicate were pooled. They are expressed in number of photoproducts per millions bases and represent mean ± standard error (n=6).*

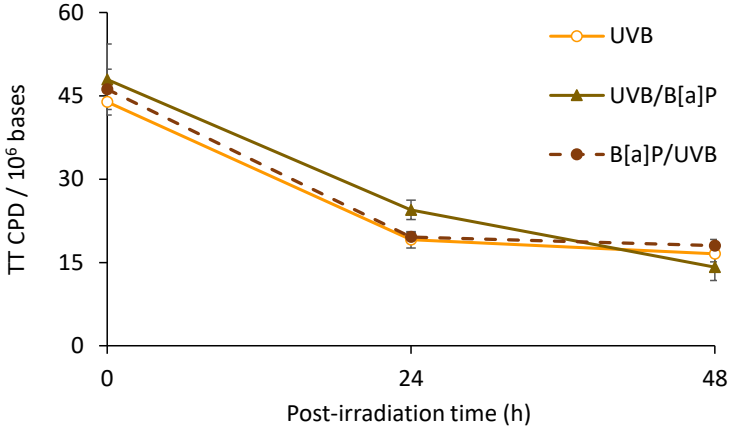

Figure S4: *Repair of TT CPD in NHK exposed to either UVB only (UVB), UVB with a subsequent B[a]P treatment performed 1 hour after irradiation (UVB/B[a]P), or UVB after a 24-hour preliminary incubation with B[a]P (B[a]P/UVB). The B[a]P concentration was 1 µM and the UVB dose 0.1 J/cm^2. Results are the mean ± standard deviation for three independent cell cultures from the same donor.*

To further characterize the effects of incubation of B[a]P prior to SSL irradiation, we performed a time-course study of the level of bipyrimidine dimers in keratinocytes from additional donors. We applied the B[a]P/SSL protocol and B[a]P was used at concentrations of both 0.1 and 1 µM, with 2 MED SSL. The impact of preliminary incubation with 0.1 µM B[a]P on repair of CPDs induced by 2 MED SSL was as significant as with 1 µM (Fig. 4). When much milder conditions were used (0.1 MED SSL and 0.1 µM B[a]P), no impact of B[a]P was observed on the repair of photoproducts (Fig. 4)

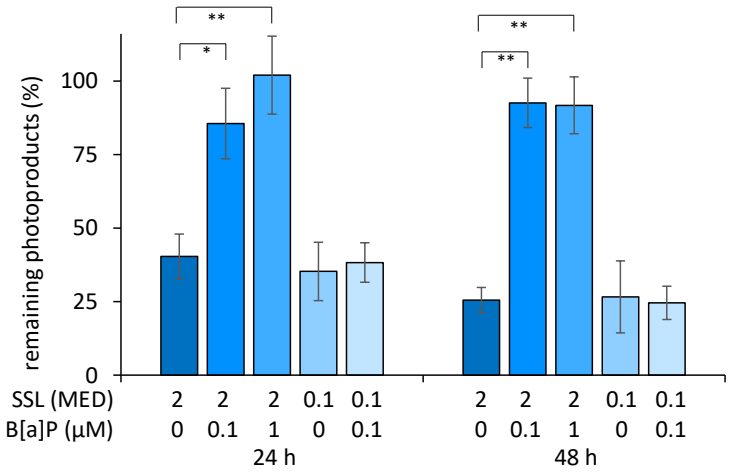

Figure 4: *Repair of CPDs in NHK exposed to SSL only or with a preliminary B[a]P treatment. Cells from a first series of 3 donors exposed to 2 MED SSL after 24 hour incubation with B[a]P at 0.1 or 1.0 µM. Cells from 2 other donors were exposed to 0.1 MED SSL with or without preliminary treatment with 0.1 µM B[a]P. Results are expressed in number of photoproducts per millions bases and represent mean ± standard error. Statistical significance with respects to SSL only *: $p<0.05$; ** $p<0.01$*

3.4 Effect of modulation of AhR on the impact of B[a]P on phototoxicity and repair of DNA photoproducts

A series of experiments were performed with the dioxin TCDD and the AhR antagonist CH223191. TCDD led to a moderate loss of viability with an average 80% MTT score (Supplementary data, Table S2), with respect to the toluene (vehicle solvent) control over the range of concentrations investigated (Fig. 5a). Toluene controls were performed together with DMSO controls. No difference in viability was detected. CH223191 exhibited no detectable effect on cell viability (Supplementary data, Table S2). The efficiency of the antagonist effect of CH223191 at the concentration used in the subsequent experiments (5 µM) was checked by measuring by HPLC-MS/MS the level of DNA adducts to the diol epoxide of B[a]P (BPDE-N^2-dGuo). As expected, the observed value was lower after 24-hour incubation in samples containing CH223191 (23.2±1.2 compared to 8.9±1.7 BPDE-N^2-dGuo per 10^6 bases with B[a]P and B[a]P+CH223191, respectively). Addition of CH223191 to B[a]P during the pre-treatment step before exposure to SSL improved neither the phototoxicity of the B[a]P/SSL protocol (Fig. 5a) nor the inhibition of DNA repair (Fig. 5b). Pre-incubation of NHK with TCDD alone did not affect the repair of photoproducts (Fig. 5b)

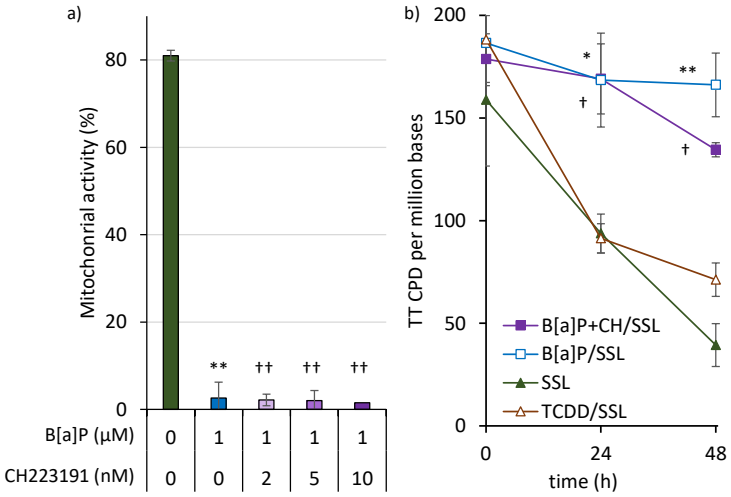

Figure 5: *Effects of the AhR agonist TCDD and AhR-antagonist CH223191 in NHK. a) Decrease in the mitochondrial activity was measured at 48 hours by performing the MTT assay in NHK exposed to SSL (2 MED) after incubation in medium containing B[a]P (1 µM) and increasing concentrations of CH223191 (CH 2, 5, and 10 µM). b) Repair of TT CPD in NHK exposed to SSL (2 MED) with or without a preliminary 24-hour incubation with either B[a]P 1 µM, B[a]P 1 µM + 5 µM CH223191 (CH), or 10 nM TCDD. Results are mean ± SEM from two donors studied in three independent cultures. Statistical significance: B[a]P/SSL vs SSL *: p<0.05; **: p<0.01; B[a]P+CH223191/SSL vs SSL †: p<0.05; ††: p<0.01*

Table S2: Mitochondrial activity measured at 48 hours by the MTT assay in NHK exposed to increased concentrations of CH223191 or TCDD. Concentrations are expressed in µM and nM, respectively. Results are expressed in % and represent the mean ± standard deviation for 3 donors (n=3) compared to vehicle-only treated controls.

concentration	2	5	10	25
CH223191 (µM)	114±10	89±24	94±13	100±12
TCDD (nM)	68±1	85±6	75±28	84±13

329

330 *3.5 Formation of 8-oxodGuo in NHK exposed to B[a]P and SSL*

331 The level of 8-oxodGuo was quantified by HPLC-MS/MS in the DNA of NHK exposed either
332 to B[a]P, SSL, the SSL/B[a]P protocol or the B[a]P/SSL protocol. Increase in the level of
333 8-oxodGuo was observed only under the latter conditions when the B[a]P concentration was 1
334 µM and the SSL dose 2 MED with a 4-fold larger value than in control NHK (Fig. 6). In
335 contrast, no significant increase was observed when the latter values were decreased to 0.1 µM
336 and 0.1 MED (2.6±0.5 and 2.9±0.6 8-oxodGuo per 10^7 bases in control and cells exposed to the
337 B[a]P/SSL protocol).

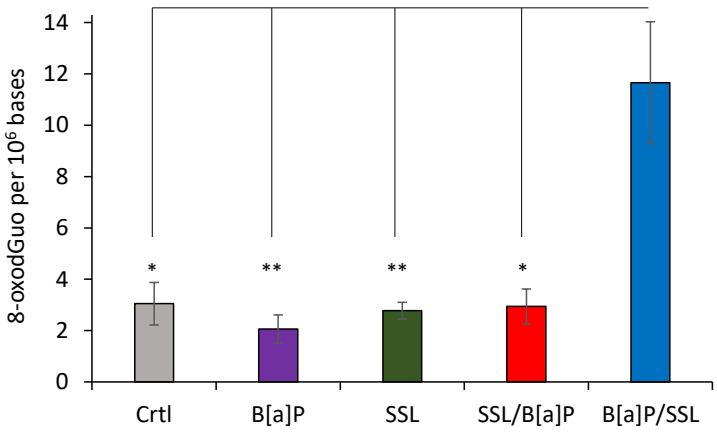

338

339 ***Figure 6:*** *Level of 8-oxodGuo in NHK exposed to 2 MED SSL, B[a]P, SSL/B[a]P and*
340 *B[a]P/SSL with or without preliminary incubation with 1 µM B[a]P for 24 hours. Controls*
341 *are non-irradiated, DMSO-treated cells. Samples were collected immediately after*
342 *irradiation. Data were obtained from two donors each studied in three independent cultures.*
343 *Results are mean ± SEM. Statistical differences with respect to B[a]P/SSL: *: $p<0.05$; **:*
344 *$p<0.01$.*

345 **4. Discussion**

346 The present study aimed at assessing whether co-exposure of normal human keratinocytes to
347 B[a]P and simulated sunlight could modulate the phototoxicity and genotoxicity of UV

radiation. We also wanted to get insights into the underlying mechanisms, specifically by determining if AhR was involved. It has been shown that, possibly under the influence of tryptophan photoproducts (Diani-Moore et al., 2006; Fritsche et al., 2007; Nair et al., 2009; Rannug et al., 1995), exposure to UV radiation increased, by a factor of approximately 5, the expression of CYP450 genes due to AhR activation (Katiyar et al., 2000; Nair et al., 2009; Rannug and Fritsche, 2006; Wei et al., 1999). Interestingly, it was recently reported that AhR exhibited a negative effect on cellular DNA nucleotide excision repair capacities (Pollet et al., 2018). Another AhR-mediated pathway for the decreased repair efficiency could be the ability to hinder mitochondrial functions and limit the production of ATP, which is essential for repair (Aly and Domenech, 2009; Chen et al., 2010; Hwang et al., 2016; Kennedy et al., 2013).

We first studied cell death either with the short-term MTT assay or on a longer time-scale by quantification of the clonogenicity of NHK. In these first experiments, the SSL dose was set at 2 MED, which corresponds to less than 1 hour of exposure on a summer day in mid-latitude in Europe with a UV index of 6. The B[a]P concentration was 1 µM which may be considered as relevant to some occupational exposures. Values as high as 100 pmol/cm^2 of B[a]P have been reported for workers in the aluminum industry (VanRooij et al., 1992). We have recently reported that the B[a]P content in skin typically exposed to complex mixtures is around 40% of the applied dose after 48h. If a penetration depth of a few hundred of micrometers, namely the epidermis and a part of the dermis, is considered, the corresponding local concentration is then the micromolar range. Cytotoxicity measured by these two complementary approaches showed that under the range of doses used, pure B[a]P and SSL only exhibited limited toxicity. When NHK were exposed to the largest SSL dose studied (2 MED) and then exposed to 1 µM B[a]P, namely the upper limit of the applied concentrations, phototoxicity was only slightly increased with respect to irradiation only. In addition, the DNA repair kinetics observed with the SSL/B[a]P protocol were similar to those obtained in cells exposed to SSL only, consistent with

the limited impact of this treatment on cell survival. These results were the same whether a delay of 1 or 8 hours was applied between exposure to SSL and B[a]P. Altogether, these observations suggest a limited impact of B[a]P on the cellular responses triggered by exposure to UV alone, and therefore a limited effect of the activation of the AhR pathway on DNA repair.

In drastic contrast to data obtained with the SSL/B[a]P treatment, the reverse protocol with incubation for 24 hours with 1 µM B[a]P followed by exposure to 2 MED SSL led to complete cellular toxicity. The same observation was made at 0.5 MED for B[a]P concentrations of 0.2 µM. At 0.1 µM, cells survived a subsequent exposure to SSL when the dose was 0.1 MED at the most. The bulk of these results shows that the incubation with B[a]P prior to irradiation strongly sensitizes NHK, unlike the reverse protocol. Similar results of a drastically increased phototoxicity by low concentrations of PAH were recently reported for fibroblasts exposed to UVA1 (Soeur et al., 2017). Our results thus show that biologically relevant doses of SSL applied after incubation with B[a]P concentration possibly found upon occupational contamination are much more toxic than the two toxic agents applied separately. It could be tempting to propose that incubation with B[a]P led to activation of the AhR pathway, which resulted in decreased DNA repair (Pollet et al., 2018) and subsequently increased cell death as the result of apoptosis triggered by high levels of DNA damage.

However, this hypothesis was the opposite of the conclusion made on the basis of the results of SSL/B[a]P protocol, which shows no effect of the co-exposure. We therefore performed a series of additional experiments to unravel the origin of the phototoxicity and the decreased DNA repair in the B[a]P/SSL experiments. We first investigated the dose effects. A low concertation of 0.1 µM B[a]P in the latter protocol induced the same effect on DNA repair as 1 µM when 2 MED SSL was applied. This result shows that the decrease in repair activity observed in the B[a]P/SSL protocol is not explained by the sole presence of B[a]P. Normal repair activity and reduced cell toxicity were observed only when both the B[a]P concentration and the SSL dose

were lowered to 0.1 µM and 0.1 MED, respectively. This result further shows that presence of both B[a]P and SSL are required for the observed effects.

In order to test the hypothesis of the involvement of AhR in the B[a]P/SSL-mediated negative impact on DNA repair, we repeated the experiments involving SSL irradiation following a 24-hour B[a]P treatment in the presence of CH223191, an AhR antagonist that would be expected to prevent repair inhibition should AhR be involved. We could not see any influence of CH223191 on the effects of the B[a]P/SSL protocol on either the mitochondrial impairment or the repair of DNA photoproducts. We performed the converse experiment by treating keratinocytes with TCDD, a dioxin that is a strong AhR agonist and should hypothetically mimic the effects of B[a]P. Results were compared with those of SSL and B[a]P/SSL protocols. TCDD did not decrease the repair rate of pyrimidine dimers after exposure to SSL. These two series of results allow us to rule out a significant contribution of AhR in the B[a]P-mediated inhibition of DNA repair. This conclusion is in agreement with the limited modulation of DNA repair gene expression and the lack of modification at the repair protein level in mouse hepatoma cell lines exposed to TCDD (Schreck et al., 2009). The fact that addition of B[a]P after irradiation, which efficiently induces AhR in NHK as shown by increased CYP450 expression and formation of DNA adducts (von Koschembahr et al., 2018), did not affect repair even 48 hours after exposure to SSL, thus further supporting a very limited role of AhR.

A more likely alternative explanation to the impact of B[a]P on UV effects could be a role of photosensitized induction of oxidative stress. This effect has been reported in several *in vitro* studies (Crallan et al., 2005; Mauthe et al., 1995; Ors and Gulce Iz, 2018; Soeur et al., 2017; Vaz Batista Filgueira et al., 2007; Xia et al., 2015; Yu et al., 2006). Accordingly, we observed a larger induction of 8-oxodGuo, a typical DNA oxidation marker, when the B[a]P/SSL protocol was applied under the most cytotoxic conditions. The decreased DNA repair activity could thus be explained by the fact that most cells are dying and metabolically inactive. The

strong phototoxicity of B[a]P has been recently documented in human fibroblasts exposed to UVA1 at concentrations of 5 and 50 nM (Soeur et al., 2017). Although these data cannot be directly compared to ours because of the difference in cell type and UV source, they illustrate the strong photosensitizing properties of B[a]P. It should be mentioned that another role of B[a]P-mediated photosensitization could be the increasingly documented negative impact of oxidative stress induced by UVA on nucleotide excision repair (Courdavault et al., 2005; Guven et al., 2015; Karran and Brem, 2016; Kimeswenger et al., 2018; Montaner et al., 2007; Mouret et al., 2006). However, the contribution of the strong loss of cell viability in NHK exposed to 1 µM B[a]P and then to 2 MED SSL is likely to be much more predominant.

A major contribution of photosensitization in our present observations would explain why the effect of B[a]P is observed only when it is added to the NHK before irradiation and not after. Involvement of a photosensitization process could also explain our observations made at 0.1 µM B[a]P. Increased phototoxicity and decreased DNA repair activity was observed when, SSL was applied at 2 MED but not 0.1 MED. If B[a]P alone was responsible for these effects, the same observations should have been made, irrespective of the SSL dose. The underlying mechanism thus clearly requires interaction between B[a]P and SSL, like in photosensitization reactions. The observation that UVB did not exhibit the same effect as SSL is another clue for the major involvement of photosensitization. Indeed, UVB is applied in a much lower physical dose than SSL and is more weakly absorbed by B[a]P, the maximum of absorption of which is in the UVA range. Therefore, UVB is expected to less efficiently induce B[a]P-mediated photosensitized processes. Our observations are reminiscent of those made in fibroblasts, where the UVA1 portion of the UV spectrum was found to be responsible for the largest part of the phototoxic and photo-oxidative effects of irradiation in the presence of PAH (Soeur et al., 2017).

5. Conclusion

Our work provides additional evidence of the possible cutaneous impacts that PAH, even in low quantities, can have when exposed to sunlight. Comparison of different protocols and specific experiments allowed us to rule out a major contribution of the AhR factor. It rather seems that the observed increase in toxicity is a classical phototoxicity reaction mediated by photosensitized-oxidative stress. In terms of risk management, this implies that extensive cleaning of skin before exposure to sunlight is an efficient safety procedure, at least as far as phototoxicity is concerned. However, it should be kept in mind that we also provided evidence that exposure to UV, applied either before or after contamination, modulated the metabolism of PAH (Bourgart et al., 2019; von Koschembahr et al., 2018). The consequences of these observations in risk management have to be further explored.

Conflict of Interest

The authors state no conflict of interest.

Acknowledgements

The authors wish to thank the team of the “Service de Chirurgie Plastique et Maxillo-faciale CHU Grenoble Alpes” for their help in skin sample collection. This work was supported by grants # ENV201411 and ENV201604 from INSERM and Plan Cancer.

References

Aly, H.A., Domenech, O., 2009. Cytotoxicity and mitochondrial dysfunction of 2,3,7,8-tetrachlorodibenzo-p-dioxin (TCDD) in isolated rat hepatocytes. Toxicology Letters 191, 79-87.

Boffetta, P., Jourenkova, N., Gustavsson, P., 1997. Cancer risk from occupational and environmental exposure to polycyclic aromatic hydrocarbons. Cancer Causes Control 8, 444-472.

Bonzini, M., Facchinetti, N., Motolese, A., Casa, M., Parassoni, D., Lega, M., Lombardo, M., Borchini, R., Ferrario, M.M., 2013. Looking for "lost occupational cancers": a systematic evaluation of occupational exposure in a case series of cutaneous squamous cell carcinomas in Italy. Medicina Del Lavoro 104, 224-235.

Bourgart, E., Persoons, R., Marques, M., Rivier, A., Balducci, F., von Koschembahr, A., Beal, D., Leccia, M.T., Douki, T., Maitre, A., 2019. Influence of exposure dose, complex mixture and ultraviolet radiation on skin absorption and bioactivation of polycyclic aromatic hydrocarbons *ex vivo*. Archives of Toxicology 93, 2165-2184.

Brash, D.E., 2015. UV signature mutations. Photochemistry and Photobiology 91, 15-26.

Brash, D.E., Rudolph, J.A., Simon, J.A., Lin, A., McKenna, G.J., Baden, H.P., Halperin, A.J., Ponten, J., 1991. A role for sunlight in skin cancer: UV-induced p53 mutations in squamous cell carcinoma. Proceedings of the National Academy of Sciences of the United States of America 88, 10124-10128.

Cadet, J., Sage, E., Douki, T., 2005. Ultraviolet radiation-mediated damage to cellular DNA. Mutation Research/Fundamental and Molecular Mechanisms of Mutagenesis 571, 3-17.

Chen, S.C., Liao, T.L., Wei, Y.H., Tzeng, C.R., Kao, S.H., 2010. Endocrine disruptor, dioxin (TCDD)-induced mitochondrial dysfunction and apoptosis in human trophoblast-like JAR cells. Molecular Human Reproduction 16, 361-372.

Cirla, P.E., Martinotti, I., Buratti, M., Fustinoni, S., Campo, L., Zito, E., Prandi, E., Longhi, O., Cavallo, D., Foa, V., 2007. Assessment of exposure to Polycyclic Aromatic Hydrocarbons (PAH) in Italian asphalt workers. Journal of Occupational and Environmental Hygiene 4, 87-99.

Courdavault, S., Baudouin, C., Charveron, M., Canguilhem, B., Favier, A., Cadet, J., Douki, T., 2005. Repair of the three main types of bipyrimidine DNA photoproducts in human keratinocytes exposed to UVB and UVA radiations. DNA Repair (Amst) 4, 836-844.

Crallan, R.A., Ingham, E., Routledge, M.N., 2005. Wavelength dependent responses of primary human keratinocytes to combined treatment with benzo[a]pyrene and UV light. Mutagenesis 20, 305-310.

Diani-Moore, S., Labitzke, E., Brown, R., Garvin, A., Wong, L., Rifkind, A.B., 2006. Sunlight generates multiple tryptophan photoproducts eliciting high efficacy CYP1A induction in chick hepatocytes and in vivo. Toxicological Sciences 90, 96-110.

Douki, T., 2013. The variety of UV-induced pyrimidine dimeric photoproducts in DNA as shown by chromatographic quantification methods. Photochemical and Photobiological Sciences 12, 1286-1302.

Esser, C., Bargen, I., Weighardt, H., Haarmann-Stemmann, T., Krutmann, J., 2013. Functions of the aryl hydrocarbon receptor in the skin. Seminars in immunopathology 35, 677-691.

Fitzpatrick, T.B., 1988. The validity and practicality of sun-reactive skin types I through VI. Archives in Dermatology 124, 869-871.

Fritsche, E., Schafer, C., Calles, C., Bernsmann, T., Bernshausen, T., Wurm, M., Hubenthal, U., Cline, J.E., Hajimiragha, H., Schroeder, P., Klotz, L.O., Rannug, A., Furst, P., Hanenberg, H., Abel, J., Krutmann, J., 2007. Lightening up the UV response by identification of the

arylhydrocarbon receptor as a cytoplasmatic target for ultraviolet B radiation. Proceedings of the National Academy of Sciences of the United States of America 104, 8851-8856.

Genies, C., Maitre, A., Lefebvre, E., Jullien, A., Chopard-Lallier, M., Douki, T., 2013. The extreme variety of genotoxic response to benzo[a]pyrene in three different human cell lines from three different organs. PLoS One 8, e78356.

Guven, M., Brem, R., Macpherson, P., Peacock, M., Karran, P., 2015. Oxidative Damage to RPA Limits the Nucleotide Excision Repair Capacity of Human Cells. Journal of Investigative Dermatology 135, 2834-2841.

Herbert, R., Marcus, M., Wolff, M.S., Perera, F.P., Andrews, L., Godbold, J.H., Rivera, M., Stefanidis, M., Lu, X.Q., Landrigan, P.J., et al., 1990. Detection of adducts of deoxyribonucleic acid in white blood cells of roofers by 32P-postlabeling. Relationship of adduct levels to measures of exposure to polycyclic aromatic hydrocarbons. Scandinavian Journal of Work, Environment & Health 16, 135-143.

Hwang, H.J., Dornbos, P., Steidemann, M., Dunivin, T.K., Rizzo, M., LaPres, J.J., 2016. Mitochondrial-targeted aryl hydrocarbon receptor and the impact of 2,3,7,8-tetrachlorodibenzo-p-dioxin on cellular respiration and the mitochondrial proteome. Toxicology and Applied Pharmacology 304, 121-132.

Karran, P., Brem, R., 2016. Protein oxidation, UVA and human DNA repair. DNA Repair (Amst) 44, 178-185.

Katiyar, S.K., Matsui, M.S., Mukhtar, H., 2000. Ultraviolet-B exposure of human skin induces cytochromes P450 1A1 and 1B1. Journal of Investigative Dermatology 114, 328-333.

Kennedy, L.H., Sutter, C.H., Leon Carrion, S., Tran, Q.T., Bodreddigari, S., Kensicki, E., Mohney, R.P., Sutter, T.R., 2013. 2,3,7,8-Tetrachlorodibenzo-p-dioxin-mediated production of reactive oxygen species is an essential step in the mechanism of action to accelerate human keratinocyte differentiation. Toxicological Sciences 132, 235-249.

Kimeswenger, S., Dingelmaier-Hovorka, R., Foedinger, D., Jantschitsch, C., 2018. UVA1 impairs the repair of UVB-induced DNA damage in normal human melanocytes. Experimental Dermatology 27, 276-279.

Marrot, L., 2018. Pollution and Sun Exposure: A Dele serious Synergy Mechanisms and Opportunities for Skin Protection. Current Medicinal Chemistry 25, 5469-5486.

Mauthe, R.J., Cook, V.M., Coffing, S.L., Baird, W.M., 1995. Exposure of mammalian cell cultures to benzo[a]pyrene and light results in oxidative DNA damage as measured by 8-hydroxydeoxyguanosine formation. Carcinogenesis 16, 133-137.

Melnikova, V.O., Ananthaswamy, H.N., 2005. Cellular and molecular events leading to the development of skin cancer. Mutation Research 571, 91-106.

Molho-Pessach, V., Lotem, M., 2007. Ultraviolet radiation and cutaneous carcinogenesis. Current problems in dermatology 35, 14-27.

Montaner, B., O'Donovan, P., Reelfs, O., Perrett, C.M., Zhang, X., Xu, Y.Z., Ren, X., Macpherson, P., Frith, D., Karran, P., 2007. Reactive oxygen-mediated damage to a human DNA replication and repair protein. EMBO Reports 8, 1074-1079.

Mouret, S., Baudouin, C., Charveron, M., Favier, A., Cadet, J., Douki, T., 2006. Cyclobutane pyrimidine dimers are predominant DNA lesions in whole human skin exposed to UVA radiation. Proceedings of the National Academy of Sciences of the United States of America 103, 13765-13770.

Mouret, S., Charveron, M., Favier, A., Cadet, J., Douki, T., 2008. Differential repair of UVB-induced cyclobutane pyrimidine dimers in cultured human skin cells and whole human skin. DNA Repair (Amst) 7, 704-712.

Nair, S., Kekatpure, V.D., Judson, B.L., Rifkind, A.B., Granstein, R.D., Boyle, J.O., Subbaramaiah, K., Guttenplan, J.B., Dannenberg, A.J., 2009. UVR exposure sensitizes keratinocytes to DNA adduct formation. Cancer prevention research (Philadelphia, Pa.) 2, 895-902.

Ors, G., Gulce Iz, S., 2018. Cytoprotective effect of a functional antipollutant blend through reducing B a P-induced intracellular oxidative stress and UVA exposure. Turkish Journal of Biology 42, 453-462.

Pandey, H., Talukdar, A., Gangte, J.S., Gupta, S.D., Chandra, N.C., 2018. Cholesterol homeostasis and cell proliferation by mitogenic homologs: insulin, benzo-alpha-pyrene and UV radiation. Cell Biology and Toxicology 34, 305-319.

Pollet, M., Shaik, S., Mescher, M., Frauenstein, K., Tigges, J., Braun, S.A., Sondenheimer, K., Kaveh, M., Bruhs, A., Meller, S., Homey, B., Schwarz, A., Esser, C., Douki, T., Vogel, C.F.A., Krutmann, J., Haarmann-Stemmann, T., 2018. The AHR represses nucleotide excision repair and apoptosis and contributes to UV-induced skin carcinogenesis. Cell Death and Differentiation.

Rannug, A., Fritsche, E., 2006. The aryl hydrocarbon receptor and light. Biological Chemistry 387, 1149-1157.

Rannug, U., Rannug, A., Sjoberg, U., Li, H., Westerholm, R., Bergman, J., 1995. Structure elucidation of two tryptophan-derived, high affinity Ah receptor ligands. Chemistry & Biology 2, 841-845.

Ravanat, J.L., Douki, T., Duez, P., Gremaud, E., Herbert, K., Hofer, T., Lasserre, L., Saint-Pierre, C., Favier, A., Cadet, J., 2002. Cellular background level of 8-oxo-7,8-dihydro-2'-deoxyguanosine: an isotope based method to evaluate artefactual oxidation of DNA during its extraction and subsequent work-up. Carcinogenesis 23, 1911-1918.

Saladi, R., Austin, L., Gao, D., Lu, Y., Phelps, R., Lebwohl, M., Wei, H., 2003. The combination of benzo[a]pyrene and ultraviolet A causes an in vivo time-related accumulation of DNA damage in mouse skin. Photochemistry and Photobiology 77, 413-419.

Schreck, I., Chudziak, D., Schneider, S., Seidel, A., Platt, K.L., Oesch, F., Weiss, C., 2009. Influence of aryl hydrocarbon- (Ah) receptor and genotoxins on DNA repair gene expression and cell survival of mouse hepatoma cells. Toxicology 259, 91-96.

Sellappa, S., Mani, B., Keyan, K.S., 2011. Cytogenetic Biomonitoring of Road Paving Workers Occupationally Exposed to Polycyclic Aromatic Hydrocarbons. Asian Pacific Journal of Cancer Prevention 12, 713-717.

Serdar, B., Lee, D., Dou, Z.H., 2012. Biomarkers of exposure to polycyclic aromatic hydrocarbons (PAHs) and DNA damage: a cross-sectional pilot study among roofers in South Florida. BMJ Open 2.

Soeur, J., Belaidi, J.P., Chollet, C., Denat, L., Dimitrov, A., Jones, C., Perez, P., Zanini, M., Zobiri, O., Mezzache, S., Erdmann, D., Lereaux, G., Eilstein, J., Marrot, L., 2017. Photo-pollution stress in skin: Traces of pollutants (PAH and particulate matter) impair redox homeostasis in keratinocytes exposed to UVA1. Journal of Dermatological Science 86, 162-169.

Teranishi, M., Toyooka, T., Ohura, T., Masuda, S., Ibuki, Y., 2010. Benzo[a]pyrene exposed to solar-simulated light inhibits apoptosis and augments carcinogenicity. Chemico-Biological Interactions 185, 4-11.

Toyooka, T., Ibuki, Y., 2007. DNA damage induced by coexposure to PAHs and light. Environmental Toxicology and Pharmacology 23, 256-263.

Vaananen, V., Hameila, M., Kalliokoski, P., Nykyri, E., Heikkila, P., 2005. Dermal exposure to polycyclic aromatic hydrocarbons among road pavers. Annals of Occupational Hygiene 49, 167-178.

VanRooij, J.G., Bodelier-Bade, M.M., De Looff, A.J., Dijkmans, A.P., Jongeneelen, F.J., 1992. Dermal exposure to polycyclic aromatic hydrocarbons among primary aluminium workers. La Medicina del lavoro 83, 519-529.

Vaz Batista Filgueira, D.D.M., Salomao de Freitas, D.P., de Souza Vottol, A.P., Fillmann, G., Monserrat, J., Geracitano, L.A., Trindade, G.S., 2007. Photodynamic action of benzo a pyrene in K562 cells. Photochemistry and Photobiology 83, 1358-1363.

von Koschembahr, A., Youssef, A., Beal, D., Calissi, C., Bourgart, E., Marques, M., Leccia, M.T., Giot, J.P., Maitre, A., Douki, T., 2018. Solar simulated light exposure alters metabolization and genotoxicity induced by benzo[a] pyrene in human skin. Scientific Reports 8, 10.1038/s41598-41018-33031-41598.

Wei, Y.D., Rannug, U., Rannug, A., 1999. UV-induced CYP1A1 gene expression in human cells is mediated by tryptophan. Chemico-Biological Interactions 118, 127-140.

Xia, Q.S., Chiang, H.M., Yin, J.J., Chen, S.J., Cai, L.N., Yu, H.T., Fu, P.P., 2015. UVA photoirradiation of benzo a pyrene metabolites: induction of cytotoxicity, reactive oxygen species, and lipid peroxidation. Toxicology and Industrial Health 31, 898-910.

Youssef, A., von Koschembahr, A., Caillat, S., Corre, S., Galibert, M.D., Douki, T., 2018. 6-Formylindolo[3,2-b]carbazole (FICZ) is a Very Minor Photoproduct of Tryptophan at Biologically Relevant Doses of UVB and Simulated Sunlight. Photochem Photobiol 95, 237-243.

Yu, H., Xia, Q., Yan, J., Herreno-Saenz, D., Wu, Y.S., Tang, I.W., Fu, P.P., 2006. Photoirradiation of Polycyclic Aromatic Hydrocarbons with UVA Light – A Pathway Leading to the Generation of Reactive Oxygen Species, Lipid Peroxidation, and DNA Damage. International Journal of Environmental Research and Public Health 3, 348-354.

Zegarska, B., Pietkun, K., Zegarski, W., Bolibok, P., Wisniewski, M., Roszek, K., Czarnecka, J., Nowacki, M., 2017. Air pollution, UV irradiation and skin carcinogenesis: what we know, where we stand and what is likely to happen in the future? Postepy Dermatologii I Alergologii 34, 6-14.

Ziegler, A., Leffel, D.J., Kunala, S., Sharma, H.W., Shapiro, P.E., Bale, A.E., Brash, D.E., 1993. Mutation hotspots due to sunlight in the p53 gene of nonmelanoma skin cancers. Proceedings of the National Academy of Sciences of the United States of America 90, 4216-4220.